Ultramicroscopy 160 (2016) 98–109

Contents lists available at ScienceDirect

Ultramicroscopy

journal homepage: www.elsevier.com/locate/ultramic

Differential phase-contrast dark-field electron holography for strain mapping

Thibaud Denneulin*, Florent Houdellier, Martin Hÿtch

CEMES, CNRS, 29 rue Jeanne Marvig, 31055 Toulouse Cedex 4, France

ARTICLE INFO

Article history:
Received 24 June 2015
Received in revised form
30 September 2015
Accepted 6 October 2015
Available online 8 October 2015

PACS:
61.05.jp
68.37.Lp
68.60.Bs

Keywords:
Holography
Strain
Dark-field

ABSTRACT

Strain mapping is an active area of research in transmission electron microscopy. Here we introduce a dark-field electron holographic technique that shares several aspects in common with both off-axis and in-line holography. Two incident and convergent plane waves are produced in front of the specimen thanks to an electrostatic biprism in the condenser system of a transmission electron microscope. The interference of electron beams diffracted by the illuminated crystal is then recorded in a defocused plane. The differential phase recovered from the hologram is directly proportional to the strain in the sample. The strain can be quantified if the separation of the images due to the defocus is precisely determined. The present technique has the advantage that the derivative of the phase is measured directly which allows us to avoid numerical differentiation. The distribution of the noise in the reconstructed strain maps is isotropic and more homogeneous. This technique was used to investigate different samples: a Si/SiGe superlattice, transistors with SiGe source/drain and epitaxial PZT thin films.

1. Introduction

Many different forms of electron holography have been explored or imagined [1]. The *off-axis* configuration that uses a post-specimen electron biprism is the most widespread [2]. It can be easily set up in a modern transmission electron microscope (TEM) thanks to the general introduction of field emission guns. The *in-line* scheme first introduced by Gabor [3] is also still being developed. It has fewer technical requirements, though the phase reconstruction involves a sophisticated algorithm and a precise knowledge of the experimental parameters [4]. McCartney et al. [5] introduced an alternative form of electron holography. They used an electron biprism placed in the condenser aperture plane of a TEM to produce two overlapping waves which impinge on the sample. By adjusting the defocus, they were able to observe phase variations due to the interference of electron beams coming from slightly distant regions. This method was called differential phase-contrast (DPC) holography because of the similarity with the DPC method known in scanning TEM (STEM) [6]. The DPC STEM technique measures the difference of intensity between opposite parts of a segmented detector. DPC holography is also similar to the *amplitude division* technique proposed earlier by Matteucci et al. [7]. In this case, the interfering illumination was obtained with a single crystal instead of a biprism.

Here we investigated the DPC holographic technique in dark-field condition i.e. using only beams diffracted by a given set of lattice planes. Dark-field electron holographic (DFEH) methods allow the *geometric* phase of crystalline materials to be recovered, and thus can be used to investigate strain [8]. The technique was originally demonstrated using the *off-axis* configuration [9,10] and subsequently the *in-line* configuration [11]. The present method shares several aspects in common with both schemes.

Fig. 1 summarizes the different dark-field electron holographic techniques. The sample is a single crystal thin foil constituted of an unstrained reference (Ref) area with known lattice parameter and a strained region of interest (ROI), for instance, a strained layer grown by epitaxy on a substrate. In the *off-axis* mode (Fig. 1(a)), the beams diffracted by the Ref and ROI regions interfere by means of an electron biprism placed below the specimen. The strain can be obtained from the gradient of the reconstructed phase. In the *in-line* mode (Fig. 1(b)), a defocus series of dark-field images is acquired. The phase and the strain are recovered by analyzing the variations of intensity related to the change of the diffracting angle.

In the DPC holographic technique (Fig. 1(c)), two initial and overlapping waves noted $\boldsymbol{k}_1$ and $\boldsymbol{k}_2$ are produced by applying a positive voltage to the condenser biprism. When the objective lens is focussing on the exit surface of the specimen, the hologram does not contain phase variations related to the specimen. However, a

* Corresponding author.
E-mail addresses: thibaud.denneulin@cemes.fr, thibaud.denneulin@hotmail.fr (T. Denneulin), florent.houdellier@cemes.fr (F. Houdellier), martin.hytch@cemes.fr (M. Hÿtch).

http://dx.doi.org/10.1016/j.ultramic.2015.10.002
0304-3991/

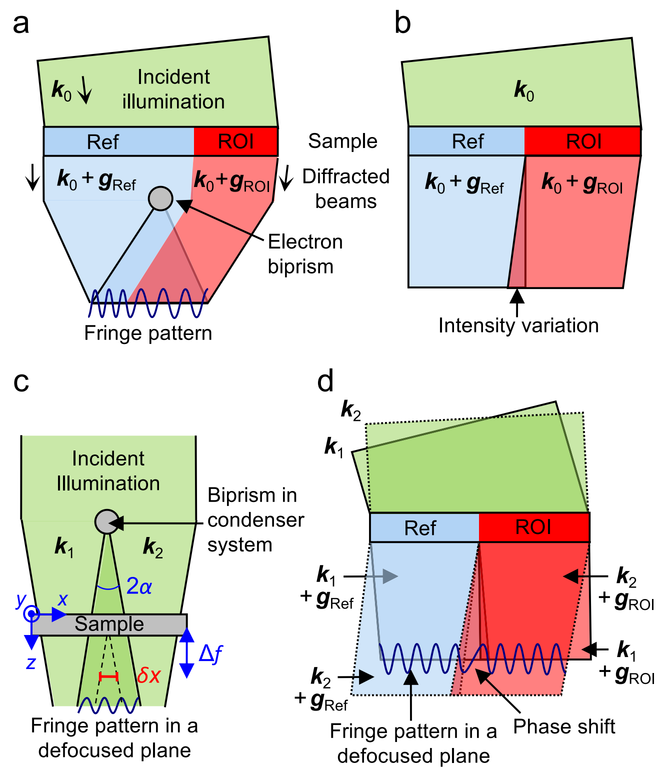

Fig. 1. (a) *Off-axis* dark-field electron holography configuration. Electron beams diffracted by the reference region (Ref) and the strained region of interest (ROI) are interfered by means of a post-specimen biprism. Hologram contains information about the difference between the interplanar distances in the two regions. Strain field can be recovered by analyzing the gradient of the phase. (b) *In-line* dark-field electron holography configuration. Changes of the diffracting angle between the reference and strained regions create a variation of intensity at the interface in a defocused plane. Phase and strain can be recovered by analyzing focal series. (c) General setup of the differential phase-contrast (DPC) holographic technique. Two overlapping waves noted $\boldsymbol{k}_1$ and $\boldsymbol{k}_2$ are produced thanks to a biprism in the condenser system. Hologram acquired in a defocused plane can be seen as a superposition of two images separated by a small distance δx. (d) DPC dark-field holography technique developed in this paper. $\boldsymbol{k}_1$ and $\boldsymbol{k}_2$ impinge on the Ref and ROI regions leading to four diffracted beams. Interference between $\boldsymbol{k}_1 + \boldsymbol{g}_{Ref}$ and $\boldsymbol{k}_2 + \boldsymbol{g}_{ROI}$ reveals a phase shift at the interface which can be interpreted in terms of strain.

small defocus allows us to image the interference of electron beams coming from slightly different regions of the sample. We note x- and y-directions respectively perpendicular and parallel to the biprism. The DPC hologram gives information about the difference between the points (x, y) and $(x + \delta x, y)$. The separation δx between the superimposed images depends on the defocus and the overlap angle 2α. The spatial resolution is also function of both the separation of the images and the holographic fringe spacing. Ideally, the separation of the images should be smaller than the resolution defined by the carrier frequency. Fig. 1(d) illustrates the DPC dark-field holographic technique (DPC-DFEH). The incident waves $\boldsymbol{k}_1 = (k_x, 0, k_z)$ and $\boldsymbol{k}_2 = (-k_x, 0, k_z)$ create four diffracted beams $\boldsymbol{k}_1 + \boldsymbol{g}_{Ref}$, $\boldsymbol{k}_1 + \boldsymbol{g}_{ROI}$, $\boldsymbol{k}_2 + \boldsymbol{g}_{Ref}$ and $\boldsymbol{k}_2 + \boldsymbol{g}_{ROI}$. In a small region around the interface, the diffracted beam $\boldsymbol{k}_1 + \boldsymbol{g}_{Ref}$ will interfere with the beam $\boldsymbol{k}_2 + \boldsymbol{g}_{ROI}$ in a defocused plane leading to a phase shift in the fringe pattern. This shift can be interpreted in terms of strain. Two diffracted beams coming from the same incident wave for instance $\boldsymbol{k}_1 + \boldsymbol{g}_{Ref}$ and $\boldsymbol{k}_1 + \boldsymbol{g}_{ROI}$ can also overlap producing a variation of amplitude at the interface similar to the scheme (b).

The intensity distribution of an electron hologram can be defined [12]

$$I(x, y) = A_1^2 + A_2^2 + 2A_1A_2\cos[\Delta\phi(x, y) + 2\pi x q_c] \tag{1}$$

with A_1, A_2 being the amplitudes, $\Delta\phi = \phi_1 - \phi_2$ the phase difference of the two diffracted waves and $q_c = 2k_x$ the carrier frequency. Considering that the regions impinged by the two waves are separated by a small distance δx in the DPC setup, the phase difference can also be written

$$\Delta\phi_{DPC}(x, y) = \phi(x + \delta x, y) - \phi(x, y) = \frac{\partial\phi(x, y)}{\partial x}\delta x \tag{2}$$

which shows that the DPC phase is sensitive to the phase derivative $\partial\phi/\partial x$ in the direction x perpendicular to the biprism. The phase information can be separated into four contributions [8]:

$$\phi = \phi_E + \phi_M + \phi_C + \phi_G \tag{3}$$

where E, M, C and G refer respectively to the electrostatic, magnetic, crystalline and geometric contributions. Here, we assume that the electrostatic, magnetic and crystalline phases are constant over the field of view, so that $\partial\phi_{E,M,C}/\partial x = 0$. The geometric phase can be defined as the extra phase term induced by a translation $\boldsymbol{u} = (u_x, u_y, u_z)$ of the reference crystal [13,8]:

$$\phi_G = -2\pi\boldsymbol{g}_{Ref}.\ \boldsymbol{u} \tag{4}$$

We will assume that this equation holds true for a varying displacement field $\phi_G(\boldsymbol{r}) = -2\pi\boldsymbol{g}_{Ref}.\ \boldsymbol{u}(\boldsymbol{r})$ (with $\boldsymbol{r}$ being the position vector in the xy plane) though this is only strictly true for small displacements [13]. If the selected $\boldsymbol{g}$-vector is perpendicular to the biprism, the DPC phase in Eq. (2) becomes

$$\Delta\phi_{DPC}(x, y) = \frac{\partial\phi_G}{\partial x}\delta x = -2\pi g_{Ref}\frac{\partial u_x(x, y)}{\partial x}\delta x = -2\pi g_{Ref}\varepsilon_{xx}(x, y)\ \delta x \tag{5}$$

where $\varepsilon_{xx} = \partial u_x/\partial x$ is the deformation of the lattice planes. The DPC phase is then proportional to both the deformation and the overlap distance δx which is proportional to the defocus. If the selected $\boldsymbol{g}$-vector is parallel to the biprism i.e. along the y